ORIGINAL ARTICLE

Diagnostic Utility of Quantifying Myocardial Flow Reserve with ^{99m}Tc-Sestamibi Dynamic SPECT Using a Standard Dual-Head SPECT Camera

Kae Fukuyama, MD, PhD[1], Yoshitoshi Kitagawa, RT[2] and Yuji Hiraoka, MD, PhD[1]

Received: April 27, 2017/Revised manuscript received: July 27, 2017/Accepted: August 1, 2017
J-STAGE Advance published: August 23, 2017

Abstract

***Background*: Quantifying the myocardial blood flow (MBF) using ^{13}N-ammonia or ^{15}O-H_2O position emission tomography (PET) is a gold standard method. However, PET MBF measurements can only be applied for limited population. A recent study showed a new myocardial uptake ratio (MUR) method. This approach may apply for the quantitative evaluation of the MBF and functional severity of the CAD. The purpose of the present study was to evaluate the diagnostic utility of the myocardial flow reserve (MFR) with this MUR method using a standard dual-head single-photon emission computed tomography (SPECT) camera.**

***Methods*: A total of 46 known or suspected CAD patients underwent adenosine stress dynamic planar acquisition following conventional ^{99m}Tc-sestamibi (^{99m}Tc-MIBI) SPECT. The area under the curve of aorta time-activity curve (TAC) was used to obtain the time integral of the first-pass ^{99m}Tc-MIBI count. The myocardial counts were obtained from SPECT short-axis images. MUR under stress and rest conditions was estimated and corrected with the cross calibration factor. Then, the MFR was calculated as the ratio of stress MUR to rest MUR.**

***Results*: The median MFR was significantly lower in patients with CAD than that without CAD (1.23 [IQR, 1.10－1.34] vs. 1.33 [IQR, 1.26－1.61], $p<0.05$).**

***Conclusions*: Patients with CAD showed significantly lower MFR using the dynamic MUR approach. Therefore, the MUR method was useful for distinguish between CAD and non-CAD patients. In this regard, MFR measurements may be useful in discerning CAD from non-CAD for the selected population.**

Keywords: ^{99m}Tc-MIBI, Dynamic SPECT, MUR method, Myocardial flow reserve
Ann Nucl Cardiol 2017；3（1）：12−19

The quantitative assessment of coronary flow reserve (CFR) may be useful for the functional evaluation of coronary artery disease (CAD). Positron emission tomography (PET) imaging is considered as the gold standard method to measure the myocardial blood flow (MBF) and CFR in a non-invasive way (1, 2). The main advantages of MBF and CFR measurements are the unmasking of “balanced ischemia” and the identification of subclinical CAD. In this regard, many reports have suggested that CFR can be a powerful independent predictor of cardiac events and mortality (3-5). However, the use of ^{15}O-H_2O and ^{13}N-ammonia requires an in-house cyclotron, and cyclotron is not equipped in many health care centers. Some studies have reported the possibilities of CFR measurements using first-pass planar scintigraphy in humans (6-9). On the contrary, recent reports have established the measurement of the MBF and myocardial flow reserve (MFR) using novel cadmium zinc-telluride (CZT) SPECT scanners (10-12). These recent SPECT technologies have been enabled to measure the MBF and MFR in clinical practice for areas where PET is not available.

^{99m}Tc-sestamibi (^{99m}Tc-MIBI) SPECT myocardial perfusion imaging is standard approach for the diagnosis of CAD. ^{99m}Tc-MIBI SPECT images are obtained by widely available standard rotating-head cameras. Even with lower spatial

doi: 10.17996/anc.17-00021

1) Kae Fukuyama, Yuji Hiraoka
Cardiovascular Center, Rakuwakai Otowa Hospital, Kyoto, Japan
E-mail: fukuyama-k@fork.ocn.ne.jp

2) Yoshitoshi Kitagawa
Department of Radiological Technology, Rakuwakai Otowa Hospital, Kyoto, Japan

Table 1a Characteristics of patients

	n=46
Age (years)	78.0 ± 6.9
Male/female	27/19
No complications	6 (13%)
DM	20 (43%)
CKD (eGFR <45)	18 (39%)
Dyslipidemia	29 (63%)

Table 1b Characteristics of patients with and without CAD

	CAD (n=25)	non-CAD (n=9)	clinical non-CAD (n=21)
Age (years)	77.8 ± 6.8	77.7 ± 7.2	78.3 ± 7.2
Male/female	18/ 7	3/ 6	9/ 12
DM	12 (48%)	5 (56%)	8 (38%)
CKD (eGFR <45)	11 (44%)	1 (13%)	7 (33%)
Dyslipidemia	18 (72%)	5 (56%)	11 (52%)

Values are expressed as mean ± SD or No. (%) of patients.
CAD: Coronary artery disease, CKD: Chronic kidney disease, DM: Diabetes mellitus
eGFR: Glomerular filtration rate

resolution and higher noise, it may still be capable of MBF quantification using a similar dynamic data acquisition. Ito et al. measured the MBF and MFR with both ^{99m}Tc-MIBI and ^{15}O labeled water PET studies in CAD patients and normal subjects. They showed a good correlation between the MFR values measured by ^{99m}Tc-MIBI and PET. However, MFR using ^{99m}Tc-MIBI was underestimated at higher flow rate (8). Komuro et al. reported a new method to calculate the myocardial uptake ratio (MUR) related with MBF quantification (13). They used the area under the curve of aorta time-activity curve (TAC) as the reference count. They obtained the myocardial counts from the SPECT short-axis view and corrected with cross calibration factor. Using input function and corrected myocardial counts, the authors calculated the MFR as the ratio of rest MUR to vasodilator stress MUR. They also suggested the stable measurements using the effective half-life correction and ordered subset expectation maximization (OSEM). They evaluated the MFR in 29 normal subjects and only one patient with 3 vessel CAD, one with chronic heart failure. They did not examined in patients who have history of CAD or various coronary risk factors. Therefore, it is not clear whether this MUR approach has clinical utility.

The aim of this study was to evaluate the diagnostic utility of MFR measurement using the new MUR method with ^{99m}Tc-MIBI SPECT studies.

Methods

Study population

We retrospectively included 46 patients who underwent adenosine stress dynamic planar acquisition following conventional SPECT imaging between December 2015 and March 2017 at our hospital (27 males, 19 females; 78.0 ± 6.9 years old). Twenty patients had diabetes mellitus (DM), and 18 patients had chronic kidney disease (CKD) with estimated glomerular filtration rate (eGFR) <45 ml/min, 29 patients had dyslipidemia (Table 1a). CAD group (n=25) was defined as patients who had significant coronary stenosis (>70%) (14) based on coronary angiography (CAG) or CT angiography (CTA) within 1 years before the SPECT study. Twenty three patients had previous coronary revascularization including coronary artery bypass grafting (CABG) (n=10). Non-CAD group (n=9) was defined as patients with no organic stenosis based on CAG or CTA within 2 years before the SPECT study. Patients with non-ischemic cardiomyopathy and vasospastic angina were excluded. Additionally, we considered 21 patients with normal SPECT and no previous revascularization, no symptoms, as the clinical non-CAD group. Clinical non-CAD group included non-CAD group (n=9) diagnosed based on CAG or CTA, and other patients diagnosed based on normal SPECT. Comparison between the clinical characteristics of patients with and without CAD are addressed in Table 1b. The local ethics committee of our hospital approved the study protocol.

^{99m}Tc-MIBI imaging protocol

All patients underwent 1-day adenosine stress and rest imaging protocol. Adenosine was infused at a rate of 0.14 mg/kg/min for 5 min (15). Three minutes after the start of adenosine infusion, ^{99m}Tc-MIBI (FUJIFILM RI Pharma Co., Ltd., Tokyo, Japan) (330 MBq) was injected intravenously as a bolus followed by flushing with 20 ml saline. Dynamic images were acquired for 2 min at a rate of 1 frame per second using the anterior planar view (13). A standard gated-SPECT scan was started 40-60 min after dynamic image acquisition. The planar dynamic images were used to estimate dynamic counts of blood pool activities, whereas SPECT images were used to estimate myocardial counts. In terms of rest dynamic acquisition, ^{99m}Tc-MIBI (660 MBq) was infused after 1 min pre-scan to obtain a baseline image of the aorta and used to subtract the residual stress counts from the aorta TAC. Pre-dynamic image was acquired for 20 sec before rest dynamic image acquisition, which was used to calculate the effective half-life for decay correction. The complete imaging protocol is shown in Fig. 1a.

SPECT imaging was performed with a dual-head gamma camera (e. cam Signature; Toshiba, Tokyo, Japan) with a low/medium-energy general-purpose collimator. The projec-

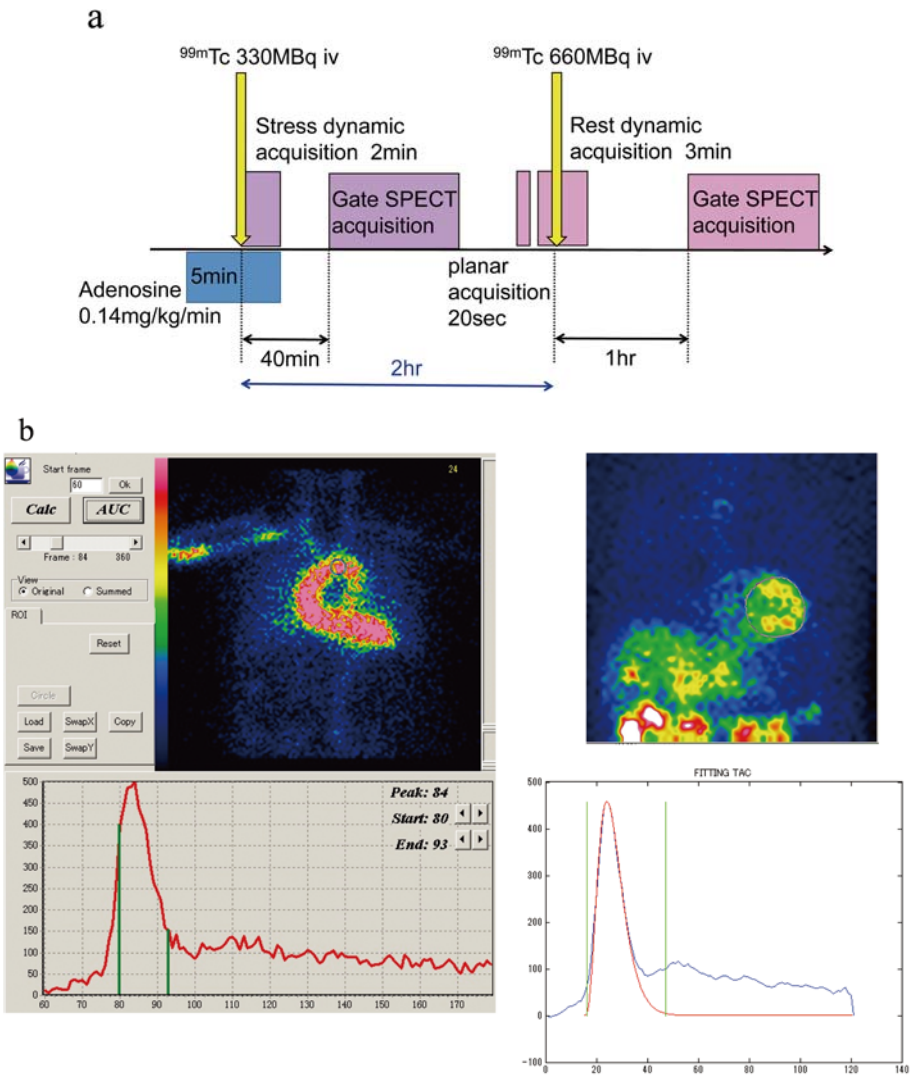

Fig. 1　**a**: Study protocol for dynamic planar acquisition following conventional SPECT imaging. **b**: TAC of the aorta and ROIs.

a: Dynamic planar acquisition is acquired for 2 min and conventional gated SPECT is performed for 20 min at both stress and rest condition. Pre-dynamic image is acquired for 20 sec before rest dynamic image acquisition to estimate effective half-life.

b: ROI was positioned on the ascending aorta and TAC was obtained automatically (left panel). Gamma-variate-fitted curve (red line) was derived and used to obtain the AUC (right lower panel). The left ventricular ROI was delineated manually (right upper panel).

AUC: area under the curve, ROI: region of interest, TAC: time activity curve

tion data was prefiltered with a two-dimensional Butterworth filter (order 8, cutoff frequency 0. 45 cycles/cm) and reconstructed with filtered back projection (FBP) and no attenuation correction. The spatial resolution of the system was 10.3mm.

^{99m}Tc-MIBI visual assessment

Regional ^{99m}Tc-MIBI uptake was assessed using the 17-segment model and semiquantitative scoring system of defect severity and extent. A commercially available software (Heart Risk View-S in AZE Virtual Place Hayabusa, AZE Co., Tokyo, Japan) was used for the semiquantitative assessment.

MFR estimation

We used cardioBull software ver. 5.1.4 and MIBI MPR software (FUJIFILM RI Pharma Co., Ltd., Tokyo, Japan) to estimate the MFR as previously described (13). Briefly, the polar map was generated from SPECT short-axis images. The myocardial count (Cmc) was obtained from these SPECT images. Region of interest (ROI) was set on the ascending aorta and the area under the curve (AUC) of γ-variate-fitted aorta time-activity curve (TAC) was used as the reference count (Fig. 1b). MUR was obtained using the formula:

MUR=Cmc/AUC×100

Whereas the Cmc is obtained from the SPECT image, AUC is obtained from the planar image and there is a geometric

Table 2a Estimated MFR with or without CAD

	CAD (n=25)	non-CAD (n=9)	p value
MFR	1.226 (1.097－1.342)	1.325 (1.260－1.610)	0.037

Table 2b The global MFR with CAD compared with clinical non-CAD group

	CAD (n=25)	clinical non-CAD (n=21)	p value
MFR	1.226 (1.097－1.342)	1.374 (1.260－1.830)	0.005

CAD: Coronary artery disease, MFR: Myocardial flow reserve

mismatch, thus Komuro et al. used the cross calibration factor (CCF) to correct the mismatch (13). CCF was estimated by the phantom experiment.

MUR=Cmc × CCF/AUC × 100

The left ventricular ROI was delineated manually on the planar image (Fig. 1b). The effective half-life was calculated using the left ventricular count of planar images at stress and rest. Myocardial count at rest condition was calculated after subtraction of the residual stress count and effective half-life. Then, the true polar map of rest MUR was generated. The MFR was calculated as the ratio of rest MUR to stress MUR.

Statistics

All statistical analyses were performed using BellCurve for Excel version 2.11 (Social Survey Research Information Co., Tokyo, Japan). Continuous values were expressed as mean ± SD and tested using a two-sample *t*-test. Non-continuous values were expressed as median with interquartile range (IQR) and analyzed using the Mann-Whitney test, with the statistical significance set at <0.05.

Results

Adenosine stress ^{99m}Tc-MIBI imaging

All patients completed the adenosine stress study without major side effects. No patient had chest pain or severe chest discomfort during adenosine infusion. With adenosine stress, there were significant increases in heart rates (66.3 ± 10.7 vs. 73.1 ± 12.2 bpm, $p < 0.001$), and significant decreases in systolic blood pressures (128.4 ± 21.5 vs. 106.3 ± 20.8 mmHg, $p<0.001$). No significant differences were found in diastolic blood pressures (59.9 ± 10.4 vs. 57.7 ± 12.9 mmHg, p=0.25). Decrease in systolic blood pressure resulted in significant rate-pressure product reduction with adenosine stress (8518 ± 1994 vs. 7752 ± 1888, $p<0.01$).

Quantitative analysis

The estimated MFR values of patient with or without CAD are summarized in Table 2a, and the box-and-whisker plots of global mean MFR values are shown in Fig. 2a. The MFR was significantly lower in CAD group than that in non-CAD group (1.23 [IQR, 1.10－1.34] vs. 1.33 [IQR, 1.26－1.61], $p<0.05$, mean ± SD: 1.25 ± 0.25 vs. 1.52 ± 0.38). Also the MFR in CAD group was significantly lower than that in clinical non-CAD group (1.23 [IQR, 1.10－1.34] vs. 1.37 [IQR, 1.26－1.83], $p<0.01$, mean ± SD: 1.25 ± 0.25 vs. 1.52 ± 0.35) (Table 2b and Fig. 2b).

Multi vessel disease

The global mean MFR of 1 vessel disease (n=20) to those of 2-3 vessel disease (n=5) in the CAD group was compared. The MFR of multi vessel patients was significantly lower than that of 1 vessel patients (1.10 [IQR, 1.00－1.15] vs. 1.27 [IQR, 1.12－1.37], $p<0.05$, mean ± SD: 1.06 ± 0.15 vs. 1.30 ± 0.25) (data not shown). Two of the 46 patients had no defect or slight abnormal accumulation in the SPECT image but had low MFR, which who were revealed to have multi vessel disease on CAG later. In Fig. 3, we showed a case with multi vessel disease (3a, 3b) and a case without coronary stenosis (3c, 3d).

Discussion

Quantifying the MFR will play an important role in the diagnosis of patients with CAD as well as risk stratification for cardiac events and mortality (4, 5). Balanced multi vessel CAD creates a diagnostic dilemma for the nuclear medicine physician. Transient ischemic dilatation (TID) score (16, 17), decrease in post-stress LV ejection fraction (18), and increased post-stress end-systolic and/or end-diastolic volume (17) may help to identify balanced ischemia; however, the utility of these markers is limited. Estimated MBF and MFR values can be additional markers to help the physician in the diagnosis.

Earlier studies suggested the possibility of quantifying the MFR on dynamic planar acquisition following conventional SPECT acquired with conventional SPECT cameras (6, 8, 9). Furthermore, several reports showed the feasibility of quantifying the MFR with novel CZT SPECT cameras (10-12). Despite the advantage of using CZT cameras for estimating the MFR value, including high sensitivity and high resolution, it is still hard to equip these CZT systems in most clinical hospitals because of its high facility cost. Estimating the MFR with the standard dual-head SPECT cameras and common ^{99m}Tc-tracers would increase the utility of MFR

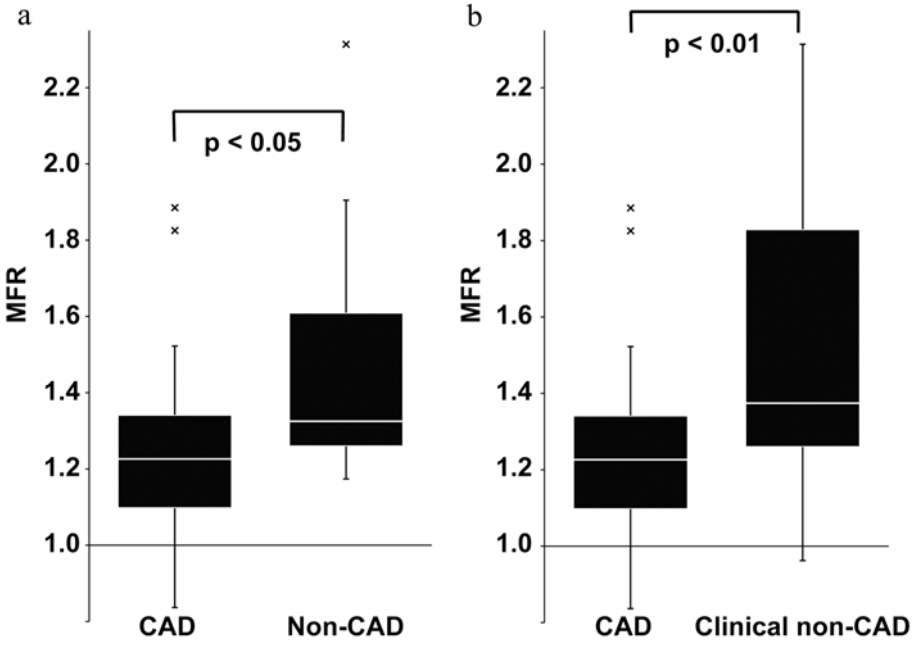

Fig. 2 **a**: Global MFR in patients with and without CAD. **b**: Global MFR in patients with CAD compared to the MFR in clinical non-CAD group.

Results are expressed as box-and whisker plots. The central box covers the IQR, with the median indicated by the line within the box. The whiskers extend to the most extreme values within 1.5 IQRs.

CAD: Coronary artery disease, Clinical non-CAD: patients without CAD based on CAG, CTA or normal SPECT, MFR: Myocardial flow reserve, Non-CAD: patients without CAD based on CAG or CTA

measurement in the clinical setting.

In the present study, we used the new MUR method for estimating the MFR in patients and obtained the acceptable values (6, 19). Ito et al. reported similar method to estimate MBF and MFR using planar and SPECT imaging based on the microsphere method (8). They used planar static image for calculating myocardial count and estimated MFR, while we used SPECT short axis view and corrected with the CCF in this new MUR method. They used 2-day rest and stress imaging protocol, however, we underwent 1-day stress and rest protocol which is much more common and clinically available. In addition, this new MUR method used effective half-life for decay correction, which was more stable than using physical half-life as previously described (13). The MFR in patients with known CAD and suspected CAD was lower than that in patients without CAD. We also examined the regional MFR in 5 segments of CAD patients and analyzed the correlation between the MFR and SPECT abnormalities, however, there was no correlation. We compared the global mean MFR of 1 vessel disease to those of 2-3 vessel disease patients. The MFR of 1 vessel disease patients was significantly higher than that of multi vessel disease, which was compatible with earlier studies (12, 20). In this study, 10 of the CAD group (n=25) had a history of CABG, and 5 of the CAD group had a history of myocardial infarction with fixed perfusion defects in the SPECT, which may affect significantly to the MFR values and complicated the results.

In our study, 2 of the 46 patients were revealed to have significant multi vessel disease after the SPECT study. They did not have abnormal accumulation in the SPECT image but had low MFR values. These results suggested that quantifying the MFR can give us an important implication for diagnosis and, especially, risk prediction in patients with suspected CAD.

Various coronary risk factors, such as CKD, DM, dyslipidemia and current smoking are known to reduce the MFR due to microvascular dysfunction (21, 22). We also analyzed the MFR in patients with CKD, DM, and dyslipidemia in non-CAD group, which was tended to lower than that of patients who did not have neither risk factors nor CAD (data not shown). We did not examine normal healthy subject in this study, thus we could not confirm relevance of these risk factors and the MFR reduction. Earlier study showed the significant difference between the MFR of diabetic CAD patients and that of non-diabetics using a hybrid SPECT/CT camera (23). Moreover, they showed the association between age, sex, smoking habit, and reduced MBF. Therefore, we strongly suggest an importance of MFR estimation to reveal the extent of CAD, detect microvascular disease and improve patient risk stratification.

The limitations in this study is that ^{99m}Tc-tracers have limited extraction fraction at high flow rates, which results in

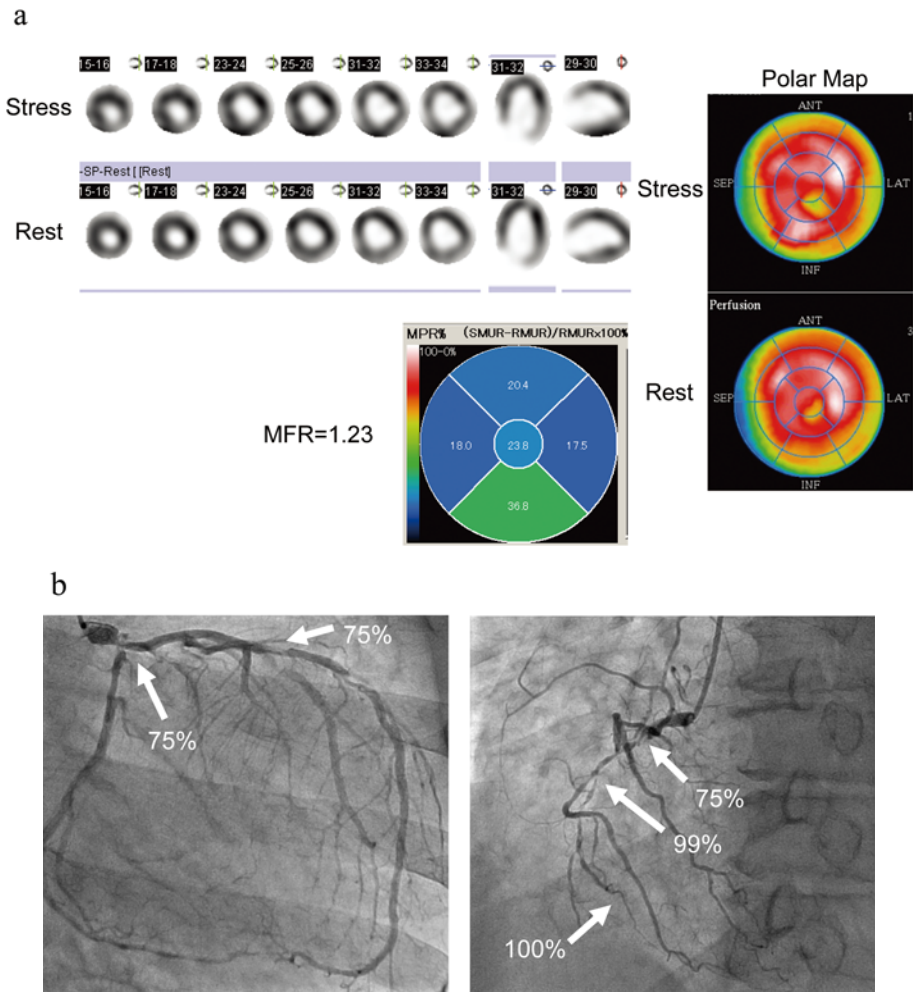

Fig. 3a, b: SPECT and coronary angiography images of 65-year-old man with 3-vessel coronary stenosis. Gated-SPECT and polar map show a slightly reduced uptake in apical inferior segment with minimal reversibility. Regional MFR values are displayed in 5-segment polar maps. Global mean MFR was reduced as 1.23.

the underestimation of the MFR value with SPECT, compared to that with PET or Doppler flowire (7, 8). Second, we categorized clinical non-CAD group which include 9 non-CAD patients proved by CAG or CTA and 12 patients diagnosed only by the normal SPECT. In this 12 patients, balanced ischemia might have been involved and there is a risk of contamination. Additionally, the interval between CAG or CTA and SPECT study in 9 non-CAD patients was up to 2 years, so that a new stenotic lesion might have progressed during this 2 years. Since there is another risk of contamination in this 9 non-CAD patients. Third, we did not correct the baseline flow values for the rate-pressure product, thus our data was highly variable compared to other studies (8, 9). Forth, we need to acquire the image for 4 times in this protocol, which may interfere throughput of the test. Therefore, it is hard to apply this method routinely in most of the patients. We suggest this dynamic planar acquisition following conventional SPECT imaging for the patients who have severe LV dysfunction without previous CAD, diffuse hypokinesis with multiple risk factors.

Further studies, on a larger patient cohort, using this MUR analysis method would still be needed. We strongly believe that the estimation of the MFR is a powerful tool and is helpful in the improvement of diagnosis.

Conclusions

The MFR can be accurately estimated with the broadly available SPECT technologies, and the new MUR method is useful for distinguish between CAD and non-CAD patients. This MUR method will contribute to the widespread use of quantitative MFR in the clinical setting.

Acknowledgments

This work was partly supported by Mr. Satomi Teraoka of FUJIFILM RI Pharma Co., Ltd. for supplying and setting the dynamic analysis software.

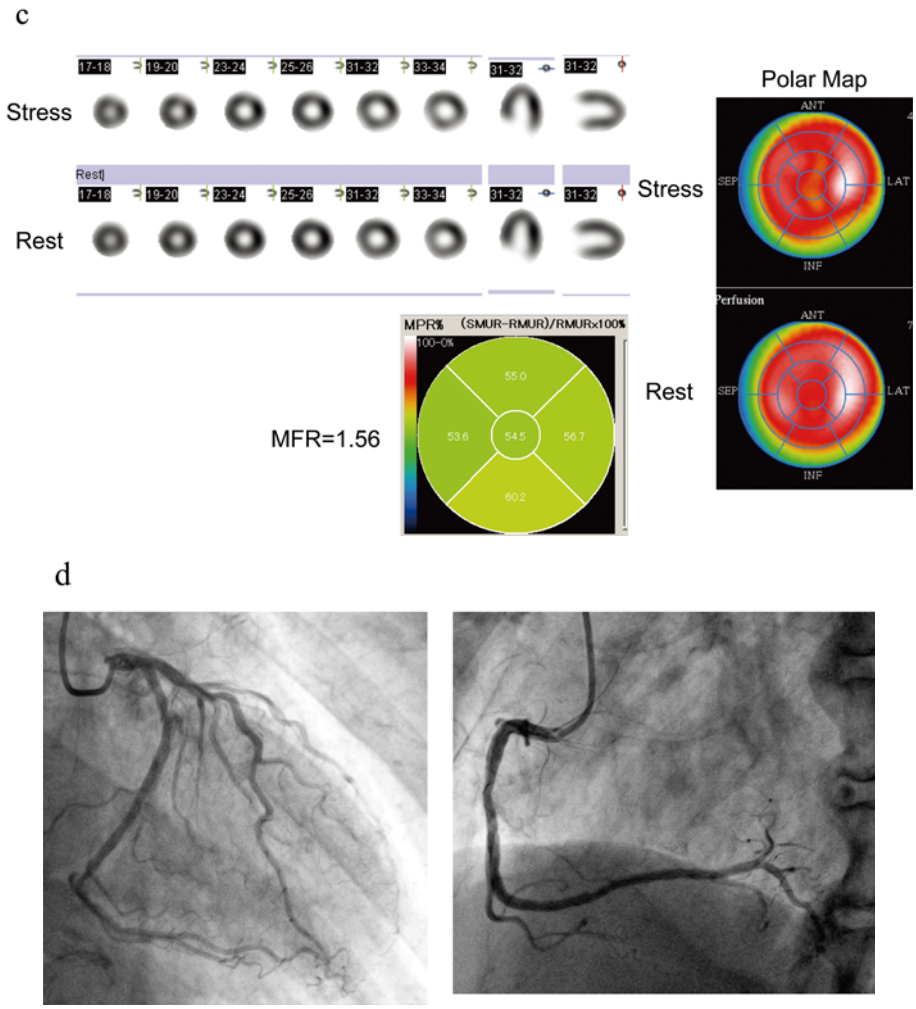

Fig. 3c, d: SPECT and coronary angiography images of 84-year-old man with no vessel stenosis. Gated-SPECT and polar map shows normal accumulation and MFR values. Global mean MFR was preserved as 1.56.

Sources of funding

None.

Conflicts of interest

None.

Reprint requests and correspondence:
Kae Fukuyama, MD, PhD
Cardiovascular Center, Rakuwakai Otowa Hospital, 2 Otowa Chinji-cho, Yamashina-ku, Kyoto City, Kyoto 607-8062, Japan
E-mail: fukuyama-k@fork.ocn.ne.jp

References

1. Bergmann SR, Herrero P, Markham J, at al. Noninvasive quantitation of myocardial blood flow in human subjects with oxygen-15-labeled water and positron emission tomography. J Am Coll Cardiol 1989; 14: 639-52.
2. Schindler TH, Schelbert HR, Quercioli A, et al. Cardiac PET imaging for the detection and monitoring of coronary artery disease and microvascular health. JACC Cardiovasc Imaging 2010; 3: 623-40.
3. Herzog BA, Husmann L, Valenta I, et al. Long-term prognostic value of 13N-ammonia myocardial perfusion positron emission tomography added value of coronary flow reserve. J Am Coll Cardiol 2009; 54: 150-6.
4. Murthy VL, Naya M, Foster CR, et al. Improved cardiac risk assessment with noninvasive measures of coronary flow reserve. Circulation 2011; 124: 2215-24.
5. Naya M, Tamaki N, Tsutsui H. Coronary flow reserve estimated by positron emission tomography to diagnose significant coronary artery disease and predict cardiac events. Circ J 2015; 79: 15-23.
6. Sugihara H, Yonekura Y, Kataoka K, et al. Estimation of coronary flow reserve with the use of dynamic planar and SPECT images of Tc-99m tetrofosmin. J Nucl Cardiol 2001; 8: 575-9.
7. Storto G, Cirillo P, Vicario ML, et al. Estimation of coronary flow reserve by Tc-99m sestamibi imaging in patients with coronary artery disease: comparison with the results of

intracoronary Doppler technique. J Nucl Cardiol 2004; 11: 682-8.
8. Ito Y, Katoh C, Noriyasu K, et al. Estimation of myocardial blood flow and myocardial flow reserve by ^{99m}Tc-sestamibi imaging: comparison with the results of [^{15}O]H_2O PET. Eur J Nucl Med Mol Imaging 2003; 30: 281-7.
9. Klein R, Hung GU, Wu TC, et al. Feasibility and operator variability of myocardial blood flow and reserve measurements with ^{99m}Tc-sestamibi quantitative dynamic SPECT/CT imaging. J Nucl Cardiol 2014; 21: 1075-88.
10. Ben-Haim S, Murthy VL, Breault C, et al. Quantification of myocardial perfusion reserve using dynamic SPECT imaging in humans: a feasibility study. J Nucl Med 2013; 54: 873-9.
11. Miyagawa M, Nishiyama Y, Kawaguchi N, et al. Estimation of myocardial flow reserve using a Cadmium-Zinc-Telluride (CZT) SPECT in patients with multi-vessel coronary artery disease. J Nucl Med 2013; 54: 517.
12. Shiraishi S, Sakamoto F, Tsuda N, et al. Prediction of left main or 3-vessel disease using myocardial perfusion reserve on dynamic thallium-201 single-photon emission computed tomography with a semiconductor gamma camera. Circ J 2015; 79: 623-31.
13. Komuro A, Teraoka S, Hosoya T, et al. Development of a new uptake ratio measurement method for myocardial blood flow quantitative evaluation in myocardial perfusion SPECT. Jpn J Nucl Med Technol 2015; 35: 199-207.
14. Levine GN, Bates ER, Blankenship JC, et al. 2011 ACCF/AHA/SCAI Guideline for Percutaneous Coronary Intervention: a report of the American College of Cardiology Foundation/American Heart Association Task Force on Practice Guidelines and the Society for Cardiovascular Angiography and Interventions. Circulation 2011; 124: e574-651.
15. Henzlova MJ, Duvall WL, Einstein AJ, et al. ASNC imaging guidelines for SPECT nuclear cardiology procedures: Stress, protocols, and tracers. J Nucl Cardiol 2016; 23: 606-39.
16. Weiss AT, Berman DS, Lew AS, et al. Transient ischemic dilation of the left ventricle on stress thallium-201 scintigraphy: a marker of severe and extensive coronary artery disease. J Am Coll Cardiol 1987; 9: 752-9.
17. Heston TF, Sigg DM. Quantifying transient ischemic dilation using gated SPECT. J Nucl Med 2005; 46: 1990-6.
18. Johnson LL, Verdesca SA, Aude WY, et al. Postischemic stunning can affect left ventricular ejection fraction and regional wall motion on post-stress gated sestamibi tomograms. J Am Coll Cardiol 1997; 30: 1641-8.
19. Petretta M, Soricelli A, Storto G, et al. Assessment of coronary flow reserve using single photon emission computed tomography with technetium 99m-labeled tracers. J Nucl Cardiol 2008; 15: 456-65.
20. Ben Bouallègue F, Roubille F, Lattuca B, et al. SPECT myocardial perfusion reserve in patients with multivessel coronary disease: correlation with angiographic findings and invasive fractional flow reserve measurements. J Nucl Med 2015; 56: 1712-7.
21. Marini C, Bezante G, Gandolfo P, et al. Optimization of flow reserve measurement using SPECT technology to evaluate the determinants of coronary microvascular dysfunction in diabetes. Eur J Nucl Med Mol Imaging 2010; 37: 357-67.
22. Murthy VL, Naya M, Foster CR, et al. Coronary vascular dysfunction and prognosis in patients with chronic kidney disease. JACC Cardiovasc Imaging 2012; 5: 1025-34.
23. Apostolopoulos DJ, Kaspiri A, Spyridonidis T, et al. Assessment of absolute Tc-99m tetrofosmin retention in the myocardium as an index of myocardial blood flow and coronary flow reserve by gated-SPECT/CT: a feasibility study. Ann Nucl Med 2015; 29: 588-602.